

# Toward self-consistent angular momentum transport in pulsating massive stars

Rich Townsend

*University of Wisconsin-Madison, Department of Astronomy, 5534 Sterling Hall, 475 N. Charter Street, Madison, WI 53706*

**Abstract.** I report on preliminary results from an ongoing project that explores angular momentum transport by unstable pulsation modes in massive stars. After briefly reviewing the underlying formalism for this transport, and describing a numerical code that implements it, I present an example simulation for a  $5M_{\odot}$  model star. I show that prograde  $\ell = m = 2$  g modes, unstable due to the iron-bump  $\kappa$  mechanism, can spin down the surface layers of the star by 25% over a short ( $\sim 100$ -year) timescale. The resulting shear layer separating the surface from interior acts to switch off the  $\kappa$ -mechanism instability, providing a natural way of limiting mode amplitudes. This process may have a role to play in the mode selection mechanism of pulsating massive stars.

**Keywords:** Early-type stars; Stellar rotation; Pulsations, oscillations, and stellar seismology; Hydrodynamics

**PACS:** 97.20.Ec; 97.10.Kc; 97.10.Sj; 95.30.Lz

## INTRODUCTION

Stellar oscillations are typically regarded as a passive player on the stage of stellar evolution — the internal structure of a star determines *how* the star pulsates. However, the converse situation can also arise, where the oscillations themselves influence the internal structure of the star. This possibility was first recognized in an astrophysical context by Ando [1, 2, 3], who considered how g-mode pulsations can extract angular momentum from one part of a star and deposit it in another, modifying the star’s rotation profile over (relatively) short timescales.

Ando’s focus was mainly on massive stars, in particular the rapidly rotating Be stars [4]. However, because his work predated the discovery of the iron-bump  $\kappa$ -mechanism instability responsible for the pulsation of massive stars [see, e.g., 5, 6], it was largely inconclusive. In later studies the focus has shifted to angular momentum transport by internal gravity waves (IGWs) — essentially, g-mode transients that are damped over a crossing time. Some authors [e.g., 7, 8] have posited that the internal rotation profile of low-mass stars is governed by IGWs stochastically excited at the base of the envelope convection zone. This mechanism has been invoked in particular to explain the near solid-body rotation in the Sun’s radiative interior [e.g., 9, 10].

Recently, there has been speculation that IGWs excited at the convective core boundary may play an important role in the angular momentum evolution of massive stars [11]. However, it seems that an equally if not more efficient agent for angular momentum transport in these stars are the unstable g modes suggested by Ando, driven by the  $\kappa$  mechanism discovered in the 1990’s (see

above). In this contribution, I report on preliminary results from an ongoing project that explores this possibility in greater detail. In the following section I briefly review the underlying formalism, and I then describe a numerical code that implements it. An example simulation using the code is presented in the subsequent section, and I finish by discussing and summarizing the findings.

## FORMALISM

Zahn [12] has argued that angular momentum diffusion in massive stars is highly anisotropic, with much stronger transport in the horizontal direction than the vertical one. This leads to effectively constant angular velocity across constant-radius shells — that is, a ‘shellular’ rotation profile. The radial transport of angular momentum is then described by an advection-diffusion equation of the form

$$\frac{d}{dr} \left[ \frac{2}{3} \rho r^2 \Omega \right] = \frac{1}{r^2} \frac{\partial}{\partial r} \left[ \frac{2}{15} \rho r^4 \Omega U \right] + \frac{1}{r^2} \frac{\partial}{\partial r} \left[ \frac{2}{3} \rho \nu r^4 \frac{\partial \Omega}{\partial r} \right] - \frac{1}{r^2} \frac{\partial}{\partial r} (r^2 \mathcal{F}_J) \quad (1)$$

Here,  $\Omega(r)$  is the angular velocity of the shell at radial coordinate  $r$ ,  $U$  the meridional circulation velocity,  $\rho$  the density,  $\nu$  the radial diffusivity (turbulent plus molecular), and  $\mathcal{F}_J$  is the angle-averaged angular momentum flux associated with pulsation waves. The left-hand side of this equation represents the rate of change of angular momentum per unit volume, averaged over all solid angles. On the right-hand side, the first term represents the angle-averaged torque due to meridional circulation; the

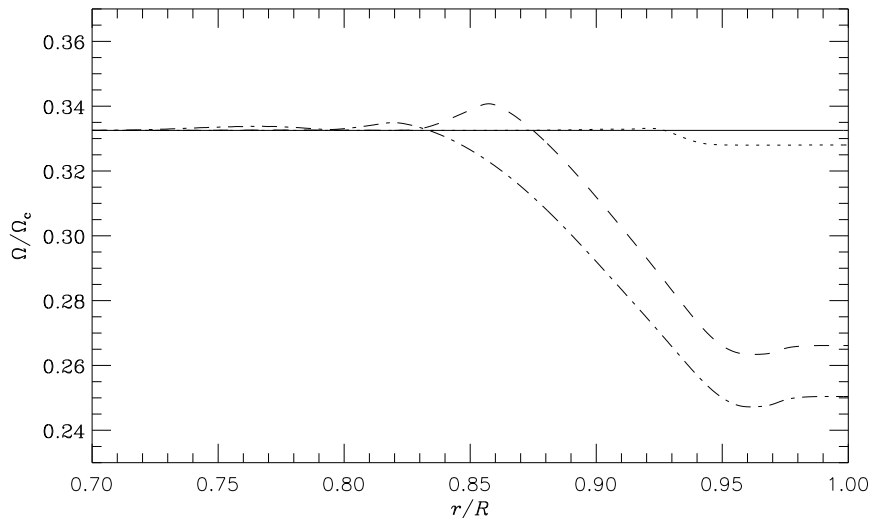


**FIGURE 1.** Snapshots of the angular velocity profile  $\Omega(r)$  during the HEIMDALL simulation. The solid line shows the initial state of uniform rotation at 33% of the critical rate  $\Omega_c$ . The dotted line plots the profile after 10 years; the dashed line after 100 years; and the dot-dashed line after 1,000 years.

second is the torque due to diffusion; and the third is the torque arising from the divergence of the wave angular momentum flux.

Lee and Saio [13] have given general expressions for the wave flux, which may be written as

$$\mathcal{F}_J = \left\langle r \sin \theta \left( \overline{\rho v'_\phi v'_r} + \overline{v_\phi \rho' v'_r} \right) \right\rangle. \quad (2)$$

Here,  $v_r$  and  $v_\phi$  are the radial and azimuthal velocity components; primes denote Eulerian perturbations; overbars indicate averages over azimuth; and angle brackets  $\langle \dots \rangle$  indicate averages over all solid angles. Inside the parentheses, the first term is the Reynolds stress, representing the radial transport of angular velocity, while the second term is the eddy mass flux, representing the radial transport of moment of inertia. This expression neglects third order terms and also the contribution of gravitational torque (which is typically small for the high-order  $g$  modes found in massive stars).

Evaluating the Eulerian-perturbed terms appearing in the expression (2) for  $\mathcal{F}_J$  requires solution of the governing pulsation equations for a differentially rotating star. I discuss a simplified approach to this solution in the following section, and describe how this is incorporated in a code for integrating the transport equation (1).

## THE HEIMDALL CODE

In [14], I introduced a new code that self-consistently models angular momentum transport by  $g$  modes. Here, I

describe the code in rather more detail, and highlight improvements since the original release. The code, HEIMDALL, evolves the angular velocity profile  $\Omega(r)$  of an otherwise-unchanging stellar model in accordance with the transport equation (1), using a first-order implicit finite-difference (backward Euler) scheme. The angular momentum transport due to meridional circulation (i.e., the first term on the right-hand side of the equation) is neglected, because it is expected to be small over the timescales on which the other terms operate. The diffusivity  $\nu$  combines contributions from radiative viscosity (typically, very small everywhere), radial turbulent viscosity (evaluated using the formalism of [15]), and convection (in convection zones, evaluated using standard mixing-length theory). Following Talon and Charbonnel [8], the diffusivity is spatially smoothed at each timestep using a Gaussian with a width equal to 0.2 times the local pressure scale height.

To evaluate the angular momentum flux via eqn. (2), HEIMDALL uses a modularized version of the BOOJUM linear, non-radial, non-adiabatic pulsation code [e.g., 16]. At each timestep, the oscillation spectrum of the star is calculated for a given set of harmonic degrees  $\ell$  and azimuthal orders  $m$ . (In a realistic simulation, *all* values of  $\ell$  and  $m$  must be included; however, in this preliminary work only a subset is considered, to simplify the analysis). The effects of differential rotation are taken into account only through the Doppler shift experienced by waves as they travel from one layer to another; the Coriolis and centrifugal forces are neglected. This is a gross simplification, but is necessary to render the pul-

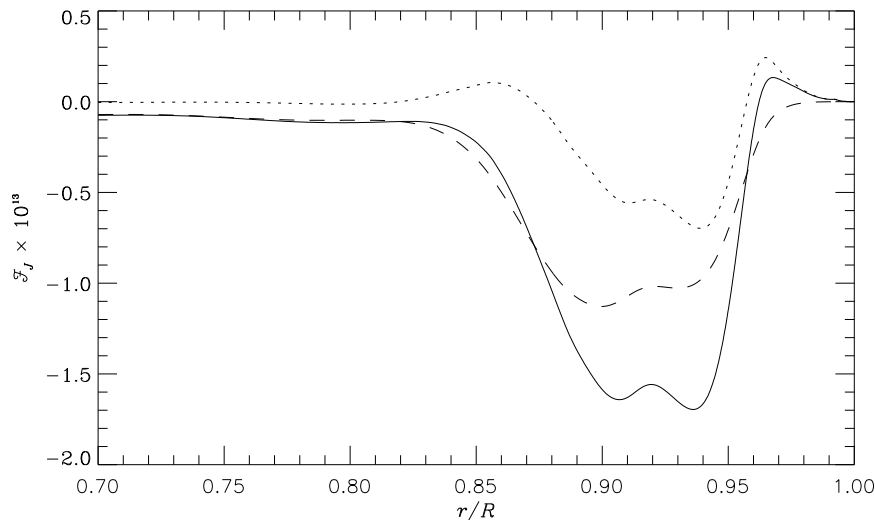


**FIGURE 2.** Snapshot of the angular momentum flux  $\mathcal{F}_J$  at 100 years into the HEIMDALL simulation, measured in units of  $GM^2/R^3$ . The solid line shows the total flux, while the dashed (dotted) line shows the contribution from the Reynolds stress (eddy mass flux) term in eqn. (2). Angular momentum is extracted where the slope of  $\mathcal{F}_J$  is positive, and deposited where the slope is negative.

sation equations solvable with modest computational effort. In this Doppler approximation, the non-adiabatic pulsation equations are identical to the non-rotating case, save for the fact that the pulsation frequency  $\omega$  is replaced by the local frequency in the co-moving frame,  $\omega_c(r) \equiv \omega - m\Omega(r)$ <sup>1</sup>.

To establish realistic values for the amplitude of each mode (which is unconstrained by linear pulsation theory), HEIMDALL assigns a small, fixed value when a mode first becomes unstable. This amplitude is then allowed to evolve across each timestep in accordance with the linear growth rate  $\gamma = -\text{Im}(\omega)$ ; as long as the mode remains unstable its amplitude will continue to grow, but if the mode ever stabilizes then its amplitude declines over time. To prevent unreasonably large amplitudes, the further growth of all modes is artificially suppressed if their combined action gives a temperature perturbation  $\langle |\delta T/T|^2 \rangle > 0.1$  in the iron-bump excitation zone. This saturation criterion was originally suggested by Dziembowski et al. [5, their eqn. 4]. However, as is discussed further in the following section, it is often the case that mode amplitudes are self-limiting by the formation of a steep shear layer, well before the saturation limit is reached.

This completes the functional description of HEIMDALL. Many of the remaining algorithms in the code are

required to ensure that the current set of excited modes can be tracked from one timestep to the next, without one or more going ‘missing’ in frequency space. This is a tricky task, and underscores the continued absence of a robust computational approach to finding the *complete* non-adiabatic pulsation spectrum of a model star.

## SIMULATION

To provide an example of HEIMDALL in action, I simulate 1,000 years of the angular momentum evolution of a  $5M_\odot$  model star<sup>2</sup> about half-way through its main-sequence evolution (i.e., lying in the center of the slowly-pulsating B (SPB) instability strip; see [17]). Starting from a state of uniform rotation at 33% of the surface critical rotation rate  $\Omega_c = \sqrt{8GM/27R^3}$ , I use HEIMDALL to evolve the angular velocity profile under the influence of prograde  $\ell = m = 2$  g modes. Fig. 1 shows snapshots of  $\Omega(r)$  taken at four stages during the simulation.

Initially, g modes with radial orders in the interval  $n = 14 \dots 34$  are unstable. These modes extract angular momentum from the near-surface iron-bump excitation zone at  $r/R \approx 0.95$ , and deposit it where they are radiatively damped in the interior (see Fig. 2). This correlation between mode excitation/damping and angular momen-

<sup>1</sup> Here, the convention is that positive (negative)  $m$  corresponds to prograde (retrograde) propagation.

<sup>2</sup> Calculated using the Warsaw-New Jersey stellar evolution code.

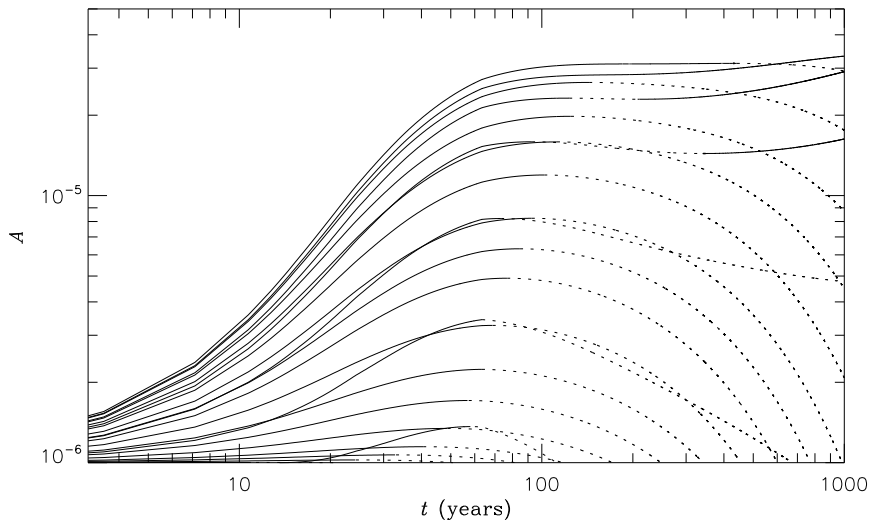


**FIGURE 3.** Time evolution of the amplitudes of the modes considered in the HEIMDALL simulation. The amplitude of a given mode is quantified as  $A = \sqrt{E}/\sqrt{GM^2/R}$ , where  $E$  is the total (kinetic plus potential) energy of the mode. Solid (dotted) lines are used to indicate modes that are growing (decaying) with time. Note that both axes are logarithmic.

tum extraction/deposition arises through the Reynolds stress term in eqn. (2), because it can be shown [e.g., 18] that this term is proportional to the differential work function.

The effects of the angular momentum transport are already visible after 10 years of simulation time, as a slight spin down in the rotation rate of the outermost layers ( $r/R \gtrsim 0.95$ ). By 100 years, this spin down is far more pronounced, because the amplitudes of the modes have grown considerably. Later still, at the 1,000 year mark, the surface layers of the star are rotating at only  $\approx 75$  percent of the interior, and the shear layer separating interior from surface has broadened, now extending from  $r/R \approx 0.85$  to  $r/R \approx 0.95$ . Of course, throughout this whole process the *total* angular momentum of the star remains unchanged; therefore, counteracting the spin down of the surface layers is a spin up of the interior, which can be seen for instance in the 100-year data as the local maximum in  $\Omega$  at  $r/R \approx 0.86$ .

In the final stages of the simulation only a few modes remain unstable, with the rest having become stabilized. This is illustrated in Fig. 3, which plots the time-evolving amplitudes of the modes contributing toward  $\mathcal{F}_J$ . At first, the amplitudes of all 21 unstable g modes increase exponentially in accordance with their initial growth rates. However, as the sub-surface shear layer develops, the  $\kappa$ -mechanism instability becomes less effective at driving the lower-order modes (for reasons discussed below). One by one, these modes transition to being stable, and their amplitudes subsequently decay with time until they contribute little toward the angular momentum flux. Af-

ter 1,000 years, only three modes ( $n = 30 \dots 32$ ) remain unstable — and for these the instability is marginal, with normalized growth rates  $\eta = -\text{Im}(\omega)/\text{Re}(\omega) \lesssim 10^{-7}$ .

Throughout this process, the artificial amplitude saturation discussed in the preceding section plays no part — the modes naturally self-limit their amplitudes through their interplay with the evolving rotating profile. As the surface layers are spun down, the co-moving pulsation frequency  $\omega_c$  in these layers becomes smaller (because the modes are prograde), and the corresponding co-moving period  $P_c$  becomes longer. This leads to the condition  $\tau_{\text{th}}/P_c \ll 1$  in the iron-bump zone (here,  $\tau_{\text{th}}$  is the local thermal timescale), and for the reasons discussed by Dziembowski et al. [5] the driving becomes ineffective. Essentially, the shear layer separating surface and interior acts as a switch that turns off the  $\kappa$ -mechanism instability.

## DISCUSSION & SUMMARY

The amplitude self-limitation described above is an intriguing result, in that it reveals a hitherto-unsuspected mechanism for mode selection in massive stars — one of the great outstanding problems in the theory of stellar non-radial pulsation. The mechanism is non-linear through the quadratic dependence of the angular momentum flux on the perturbation amplitudes (cf. eqn 2), yet can be modeled using the well-established formalism of linear pulsation. Encouragingly, the typical limiting surface velocity amplitudes encountered in the HEIMDALL

simulation — on the order of  $5 - 10 \text{ km s}^{-1}$  — are in good accordance with values inferred from observations of SPB stars.

There are some important caveats to these findings. Most significantly, the simulation presented above is typical only to prograde modes. Zonal ( $m = 0$ ) modes do not transport angular momentum because they are axisymmetric, and therefore their amplitudes cannot be self-limited in the manner described. For retrograde ( $m < 0$ ) modes, the situation is a little more complicated. If the Reynolds stress term in eqn. (2) were the only contributor toward the angular momentum flux, then retrograde modes would behave like prograde modes with the sense reversed: the surface layers would be spun up, the interior would be spun down, and the amplitude self-limitation would function in exactly the same manner.

However, inclusion of the eddy mass flux term in eqn. (2) breaks this convenient symmetry, and HEIMDALL simulations of retrograde modes (with the same stellar model and initial state) reveal mode amplitude growth until the artificial saturation is triggered. That said, if the initial rotation rate is sufficiently slow that the eddy mass flux term is small, then some kind of amplitude self-limitation for retrograde modes is conceivable. It is also possible that the Coriolis and centrifugal forces (neglected in the present analysis) may have some role to play.

Investigation of these various issues will doubtless provide fertile ground for future studies. However, the simulation presented in the present paper already makes a persuasive case that angular momentum transport by unstable  $g$  modes can lead to significant modifications to the rotation profiles of massive stars, over timescales that are quite short. Given the preeminent role that rotation plays in massive-star structure and evolution [e.g., 19], it seems likely that the pulsational transport will have far-reaching consequences.

## ACKNOWLEDGMENTS

This work has been supported by NASA LTSA grant NNG05GC36G and NSF AST grant 0908688. I'm very grateful to Wojciech Dziembowski and Stephane Mathis for fruitful discussions during the meeting.

## REFERENCES

1. H. Ando, *MNRAS* **197**, 1139 (1981).
2. H. Ando, *A&A* **108**, 7 (1982).
3. H. Ando, *PASJ* **35**, 343 (1983).
4. H. Ando, *A&A* **163**, 97 (1986).
5. W. A. Dziembowski, P. Moskalik, and A. A. Pamyatnykh, *MNRAS* **265**, 588 (1993).
6. W. A. Dziembowski, and A. A. Pamyatnykh, *MNRAS* **262**, 204 (1993).
7. S. Talon, and C. Charbonnel, *A&A* **405**, 1025 (2003).
8. S. Talon, and C. Charbonnel, *A&A* **440**, 981 (2005).
9. J.-P. Zahn, S. Talon, and J. Matias, *A&A* **322**, 320 (1997).
10. S. Talon, P. Kumar, and J.-P. Zahn, *ApJ* **574**, L175 (2002).
11. F. P. Pantillon, S. Talon, and C. Charbonnel, *A&A* **474**, 155 (2007).
12. J.-P. Zahn, *A&A* **265**, 115 (1992).
13. U. Lee, and H. Saio, *MNRAS* **261**, 415 (1993).
14. R. H. D. Townsend, and J. MacDonald, "Can Pulsational Instabilities Impact a Massive Star's Rotational Evolution?," in *Proc. IAU Symposium 250: Massive Stars as Cosmic Engines*, edited by F. Bresolin, P. A. Crowther, and J. Puls, 2008, p. 161.
15. S. Talon, and J.-P. Zahn, *A&A* **317**, 749 (1997).
16. R. H. D. Townsend, *MNRAS* **360**, 465 (2005).
17. A. A. Pamyatnykh, *Acta Astronomica* **49**, 119 (1999).
18. W. Unno, Y. Osaki, H. Ando, H. Saio, and H. Shibahashi, *Nonradial Oscillations of Stars*, University of Tokyo Press, Tokyo, 1989, 2 edn.
19. A. Maeder, and G. Meynet, *ARA&A* **38**, 143 (2000).